Visual Pathway Simulation

by

Anwer Alkaabi

A Thesis Presented to Sharif University of Technology, International Campus, Kish Island in partial fulfillment of the Requirements for the Degree of Master of Science in Computer Engineering

Supervisor: Dr. Hussain Peyvandi

Kish Island, Iran, 2020

Sharif University of Technology

International Campus, Kish Island

This is to certify that the Thesis Prepared,

By: **Anwer Alkaabi**

Entitled: **Visual Pathway Simulation**

and submitted in partial fulfillment of the requirements for the Degree of

Master of Science

complies with the regulation of this university and meets the accepted standards with respect to originality and quality.

Signed by the final examining committee:

Supervisor: _____

Co-Supervisor: _____

External Examiner: _____

Internal Examiner: _____

Session Chair: _____

AUTHOR'S DECLARATION

I declare that I am the sole author of this thesis. The work described in this thesis has not been previously submitted for a degree in this or any other university. All and any contributions by others are cited. This is a true copy of the thesis, including any required final revisions, as accepted by my examiners. I understand that my thesis may be made electronically available to the public.

Abstract

Visual Pathway Simulation

Anwer Alkaabi, M.Sc.

Sharif University of Technology, International Campus, Kish Island, 2020

Supervisor: Dr. Hussain Peyvandi

It should be a concise statement of the nature and content of the thesis. The text must be double-spaced. Abstracts should be limited to one page, when possible. No references, tables and Figures are allowed within the abstract.

Acknowledgements

Enter acknowledgements here.

Dedication

If no dedication page is included, the Table of Contents should start at page v.

Table of Contents

List of Figures

Insert List of Figures here.

List of Tables

Insert List of Tables here.

Chapter 1 Introduction

We now know that unique receptor cells are in the area, which respond to different energy sources and bind to specific nerves. Two hypotheses regarding the simultaneous processing of sensory input are well established. First of all, it is well known that sensory characteristics are provided by separate, additional processes, such as light touch toward pain and temperature, in the somatosensory system. This form of parallel mechanism applies to the visual system, and other sensory structures. Second, data from different peripheral locations in modes such as vision and audition are transmitted parallel to the brain to retain awareness of spatial location [1]. On one end of the spectrum structures, paths, components and locations of the brain may be thought of as committed to a specific function. For e.g. the rule of basic nerve energies suggests cells, pathways and areas connected to the optic nerve are associated with the sensory qualities of view. At the other hand, brain models consider tasks per network activity, in which cells perform a range of functions according to which network is involved. However, these segments are not independent but are tightly connected to a large network organizing intentional behavior. But it is still a big challenge to grasp how these neurons develop their reaction products. The learning process is defined by the manner in which neurons interact via successive stages of the visual route, driven by the rich visual input from natural scenes. This can be analyzed through the simulation of computer models that correctly model the behavior of each neuron, which alter the synaptic links between cells throughout the learning phase,

and which correlate with each neuron of the brain with the visual information's statistical properties [2].

The aim of this study is to simulate the visual pathway and to improve comprehension, however the brain may learn to interpret visual information from natural scenes. Understanding how dynamic visual scenes are perceived in the brain will help direct the clinical treatment of people with a brain and vision disorder and contribute to the introduction of new generations of vision systems.

1.1 Visual Perception

Visual perception is the ability of the brain to process and discovers images we see and where they are. Biologically, Vision begins with the eyes, but really it takes place in the brain, specifically within a region called the cerebral cortex. The brain undertakes numerous computational tasks using its network of neurons interacting with each other. These tasks are mostly performed in parallel due to the complex nature of the decision and\or outcome, however, they may also be carried out in sequence. Mainly the retina, lateral geniculate body (LGN), and visual cortex belong to the visual system. It gathers and processes visual information in order to shape perception. The cone cells and rod cells on the retina translate the light stimuli into nerve impulses and are then taken into the brain. A visual repeater in the thalamus and often a processing core is a lateral geniculate nucleus (LGN). The cortex and subcortex have reciprocal feedback and a reciprocal innervation from the visual cortex [3].

Image input from the visual region 1 (V1, Brodmann area 17) travels through the lateral Geniculate nucleus and is further transferred to areas of (V2–V5). Primary visual cortex neurons (V1) discern subtle visual, spatial, and color shifts. V1's selectivity of the object boundary orientation plays a significant role in type perception [4]. [5] suggested the development of outstanding maps by autonomous intracortical mechanisms of the primary visual cortex (V1), which would direct focus or look change, which would affect top-down selection process. The exterior appearance of a visual position explains its potential to draw interest without the top-down element. The second main region of the visual cortex (V2) is the second highest. V2 got clear V1 input and sent strong predictions to other regions of the visual cortex of the macaque brain (V3, V4, and V5).

The Receptive Area of light stimulation, which can stimulate nerve cell activity, is known as the cell's visually receptive field. [6] first suggested a concentrated circle structure receptive field. The central and peripheral discharge patterns are opposite. Both patterns are the “on” center one in which the center "on" gives the surround "off and the "off" center one in which the center "off" gives while the surrounding gives on. This structure is the classic receptive field (CRF). Following study, wider regions beyond the CRF were shown to be capable of controlling the reaction of neurons to stimuli. A considerable number of studies on the disinhibitory reaction to the grating stimuli were performed, and several useful results were achieved. Scholars also found that there is a zone around the classical receptive field, the disinhibitory area beyond the CRF, which has a disinhibitory impact upon it [7].

1.1.1 Ventral-Dorsal pathway

The propagation of information from V1 has two primary ventral pathway, and dorsal pathway networks. The ventral pathway stops at V1 through V2 and V4 and enters the lower temporal cortex. The dorsal pathway stops at V1 and travels from V2 to V5, V6. Eventually, it enters the parietal cortex behind it. The ventral pathway is related to the identification of objects, whereas the dorsal pathway is correlated with the location and action of the subject and with the regulation of the arms and eyes. While underspecified anatomically and functionally, it is essential that the sensory representations of the speech should interact with at least two structures, a motor-articulation system and a conceptual system, as a consequence of these first network ideas. The neuro-anatomic basis of this dual-pathway model was investigated by identifying cortical network nodes in both streams using functional MRI (fMRI) activations and monitoring the white matter fiber connecting these enabled nodes with a modern DTI tractography system [8]. Based on this and other analogies, a dual-stream approach for auditory language processing has been recently suggested. The mechanism diverges into two processing streams from the superior temporal gyrus, which participates in the early cortical phases of speech comprehension. The dorsal stream projects to the lower parietal and rear frontal lobe regions dorsally and includes auditory-engine convergence by translating acoustic speech sounds to articulative representations. The ventral stream projects to the central and lower time cortices and acts as an intermediary to the sound by translating sound-based speech representations to broadly scattered mental representations.

[9] indicates that selectiveness for mirror-symmetric viewing angles can constitute an intermediate processing phase shared through several high-order areas of the ventral and dorsal streams, providing the stage for full visual invariant images at subsequent visual processing levels.

1.2 Visual Processing along the Visual Pathway

Not only main sensory features direct focus during human perceptual cognition, but also intermediate and advanced vision processes. The essential task of directing the perception of artifacts and the relationship with semantic knowledge facilitates the connection of concentration with primary visual features and effects of visual processing [10]. With today's machine vision applications, the brain has the power to analyze and identify things in natural environments. The primate brain utilizes a rich cell tissue that encodes various forms of sensory input under this capability. In the retina, spatial contrasts are obtained from the two-dimensional light and color feedback of the photoreceptors in the brain as the input of visual details. The details on the spatial variations on the visual field of each position is an essential collection of features to be explored in later stages. This data is diffused through the brain cortex and combined along the visual pathway.

The visual pathway includes neurons that respond to objects/faces regardless of location, size or direction. The way these neurons establish their reaction characteristics during learning remains a mystery. Learning processes rely on the interplay of neurons across consecutive stages of the ventral visual pathway as visual feedback from natural scenes activates them.

Computer simulation is used to research how the activity of individual neurons is modeled, how the neural relations between cells during learning are changed, and how the neurons are connected in the brain. Compared to the existing machine vision technologies, the brain has remarkable capacity to identify artifacts in natural scenes. To do this the brain creates and uses a tapestry of cells that encodes different forms of visual knowledge. Photoreceptors perceive spatial contrasts from 2-dimensional light and color signals on the retina (the entrance of visual information to the brain).

The essential collection of features is the spatial contrast details at any position around the field of vision. This function is applied to the cerebral cortex and inserted into the sensory pathway. The ventral visual route thus generates neurons that respond to artifacts of complex visual type and move from plain, directed lines to whole objects or faces of the inferotemporal cortex [11]. Encoding models have been new instruments for researching human vision and neuronal pathways in recent years, allowing researchers to predict brain function dependent on stimuli. In comparison, machine vision neural networks give information into how sensory data is handled by showing a similar processing hierarchy to visual processing along the visual pathway. [12] have established a system which combines vision networks with functional MRI brain data into one model. They were able to reliably predict brain activity based on encoding models educated in brain activity and neural network features using their feature-weighted receptive field (fwRF) software.

[13] proposed that the ventral pathway is better interpreted as a recurring occipitotemporal network comprising neural representations of entity consistency both used and limited by at least six different cortical and subcortical networks.

Each mechanism serves its own specialized cognitive behavioral or affective purpose, collectively supplying the explanation for the ventral visual pathway. This extended paradigm compares with the portrayal of the ventral visual pathway as a predominantly serial staged hierarchy resulting in specific entity representations for use primarily by ventrolateral prefrontal cortex and more parsimoniously than this account, integrating attentive, qualitative and input impact.

1.3 Computational simulation

For a single topic, the simulation reads an input threshold at any point in the field of view and then uses a test protocol (ZEST, REBS, or MOBS). In the simplest mode, the simulation assumes that no signal with a lower contrast (greater decibel) than the input threshold ("no" response) can be seen. In the same manner, a 'yes' response is given to every stimulus providing a higher contrast (lower decibel) than the input threshold. When the stimulation is viewed at a level equivalent to the input threshold, a 50 percent likelihood "yes" or no" answer is selected. The test protocol is performed with these answers and the corresponding threshold is output. Comparing the resulting threshold to the input threshold tests the precision of the evaluation, whereas the amount of submissions needed is seen as an efficiency metric.

Computing modeling and computer vision technologies are particularly helpful in helping to explain the neuronal features and show the flexibility of visual circuits or pathways. These models may also be suitable modules for the design in low energy, quick and stable way of complex vision systems or sensors for potential machinery such as robots and

others. Interdisciplinary research between neuroscience and informatics has significantly encouraged the advancement of the two areas. The outcomes of these research will help people grasp the nature of biological processes, include computer platforms and intelligent methods for biological studies and increase the intelligence and efficiency of computer science algorithms. scholars claim that they correctly understand how V4 and TEO neurons grow their type selective response properties by learning.

[14] scholars studied the neuronal functions in VisNet model in a biologically plausible method, with a practical and normal picture of unsupervised competitive education and self-organization. The experiments have shown that individual network output cells can grow single, clustered, hand-centric receptive fields which are invariant for retinal locations. updated VisNet to model neuronal entity form representation in the primate ventral visual system. The individual neurons exhibit identical fire properties with V4 and TEO through unattended visually directed learning. The neurons of the higher network layer will learn to react to localized boundary contour components and to demonstrate invariances in translation across various retinal locations by using a trace learning law. The neurons of the higher network layer will learn to react to localized boundary elements and show trace-learning invariances at many retinal sites. Both machine models replicate digital path concepts and processes and will motivate future work on bio-inspired visual modeling to process images [11]. The two computer models simulate the concepts and processes of the visual pathway and may motivate potential work on bio-inspired visual modeling for the processing of photographs [15].

1.4 VisNet

Most architectural characteristics of the VisNet Model is described in [16]. VisNet consists of four competitive neural layers that have synaptic input ties between successive layers, as seen in Figure 1.

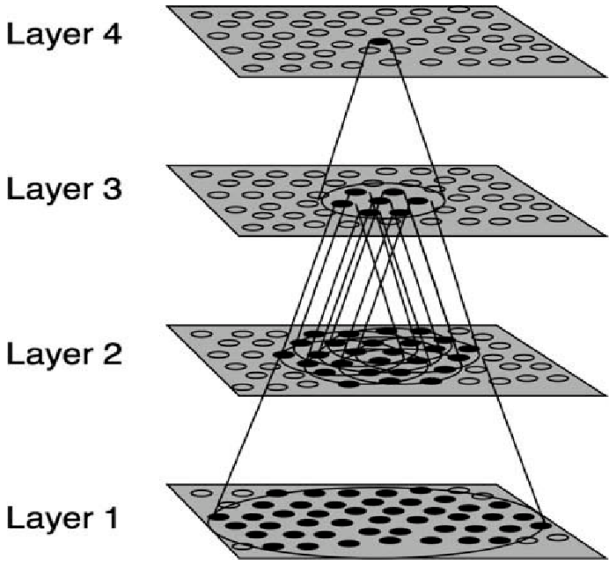

Figure 1.4.1. The VisNet neural architecture the four layers of neurons are arranged hierarchically and feedforward synaptic interactions between successive layers.

They form the foundation for the VisNet architecture and can be summarized as:

- A set of competing networks, arranged into hierarchical layers with a short range of reciprocal inhibition in each layer. These networks allow neurons to learn combinations of features or inputs that appear under a specific spatial structure utilizing competitive learning to ensure that the spatial properties of the input stimuli are reflected in the network more in order.

Layer 1 is V2, layer 2 is V4 in VisNet, layer 3 to rear lower temporal cortex and layer 4 to rear lower temporal cortex. Layer one is followed by a simulation of Gabor-like receptive fields of V1 neurons generated with each VisNet image.

- A convergent sequence of associations between the receptive field size of neurons across visual processing areas or layers in the previous layer and any of the neurons below the layer, as seen in figure 1.
- Updated (Hebb-like) associative learning rule that integrates a temporal track of the previous operation for each neuron allows the neurons to learn transforming invariance.

The VisNet architecture is feed-forward with lateral interactions within layers. There are many engineering approaches to efficiently solve similar problems extensively rely their architectures on top-down information flows, mainly for their supervised learning.

Evaluating and modeling how the visual pathways both dorsally and ventral relate to this. The dorsal visual system with LIP region is focused on graphic visual outputs which helps the eyes to fix possible items in several degrees. A four-layer hierarchic VisNet model of the ventral visual pathway transmits visual input at a position subjected to roughly the receptive fields of All that neurons.

Chapter 2 Literature Review

This chapter offers an introduction to consider new methods in visual field analysis. It outlines certain experiments, including their benefits and drawbacks, and the settings for the most effective usage of various tests. It also requires a significance measure of the visual field test. The accurate knowledge regarding the visual pathway in the modern world will provide a good basis for the creation and identification of the visual field. For this cause, explanation and observation may discuss or escape the knowledge gained by simulating the visual direction of the current scenario and possible threats contributing to weakness or lack of visions. However, it is a challenge to diagnose progressive vision deterioration since there is no independent criterion to measure the efficiency of a new system. Digital modeling models of great utility in the discovery of harmful diseases such as glaucoma, were given in many experiments. Our understanding of its neuroanatomy, functioning and external goals has evolved considerably since the first characterization of the visual pathway.

2.1 Research on Biological Vision

The vision system is a complex automatic control system, which can be studied from the perspective of cybernetics. But it not only involves eye activities, but also neural activities such as the brain stem, cerebellum, and brain. Even medically speaking, it is an interdisciplinary complex system. In terms of research methods, there are many different ways to study different aspects of the eye, including physiological and biochemical aspects, systems and information aspects, and clinical applications.

2.2 Methods of early detection

In order to allow for careful monitoring and care and mitigate the likelihood of permanent visual field loss, early identification of glaucoma is critical. Whilst advancements in ocular imaging provide the opportunity for earlier diagnoses, a mixture of knowledge from structural and functional studies is likely to be the optimal approach. [17] The new studies have shown that an assessment of the amount of retinal ganglion cells is feasible via an optical coherence tomography and normal automated calculation (CSFI). Test findings found that CSFI is more able to feel glaucoma than separate structural and functional measures which is beneficial for glaucoma before assessment.

2.3 Visual field Simulation Models

2.3.1 Retinal Simulation Platform

[18] introduced an integrated conductivity-based retina microcircuit simulator that converts light stimulation into a sequence of phototransduction graded and spiking action potentials. They used discrete retinal neuron blocks, focused on one-compartment models and morphologically accurate formulations, and succeeded in developing a simulator in real-time. This simulator includes some of the recent advancement in compartmental modelling, including five intrinsic ion currents per cell, to ensure real-time efficiency, to achieve photoreceptor rod and cone cell ion current and membrane responses, and the bipolar and amacrine cells, as well as their laterally electrical and chemical synapses, and the output ganglion cell. This study improves the work presented in [19] that introduces a retinal modeling platform incorporating the visual processing inside the vision framework

of the vertebrate, converting incoming illumination into a spike train that is sent to the brain for understanding. Retinal anatomy, from the constituent cell types to their connectivity, is generally well known, however the process of measuring subcircuits of the retina is not yet completely discerned.

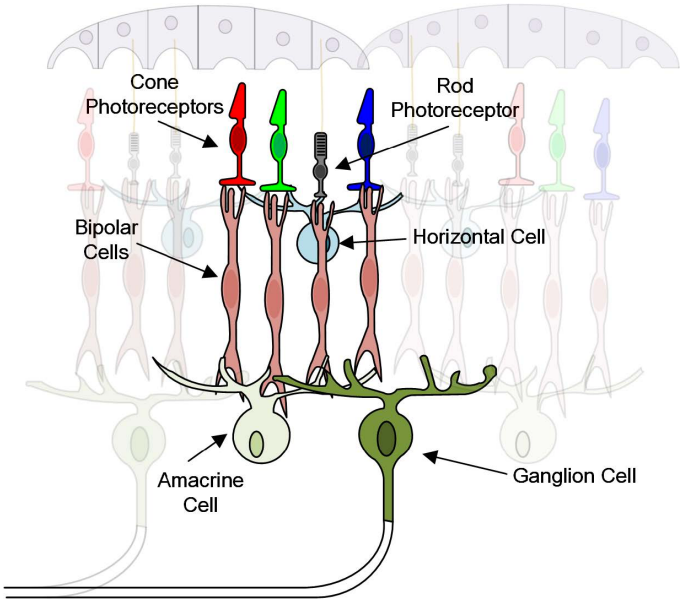

Figure 2.3.1. Dual rod and cone pathway. Light signals are converted into electric signals flowing through individual pathways from rod and cone cells and are inserted through ganglion cells that contribute to a spike.

On a larger scale, retinal neurons encode sensory input as a gradient or spiking potential and pass the effects to downstream neurons as well as to the side connections and feedback as seen in Figure 2.3.1.

particularly regarding the inability to account for the correlations, which negatively impacts the accuracy of longitudinal visual field data. In addition to that, it also mitigates the risks of uncertain validity due to the linear approach and instead proposes the implantation of nonlinear models to ensure the capturing of changes over a long period of

time. The two components required in this methodology for getting simulation were longitudinal approximations of accurate visual sensitivity over time and estimates of the noise components. For measuring the visual sensitivity, a sigmoid regression model was used at threshold sensitivities of each location, similar to the method used in [19]. However,

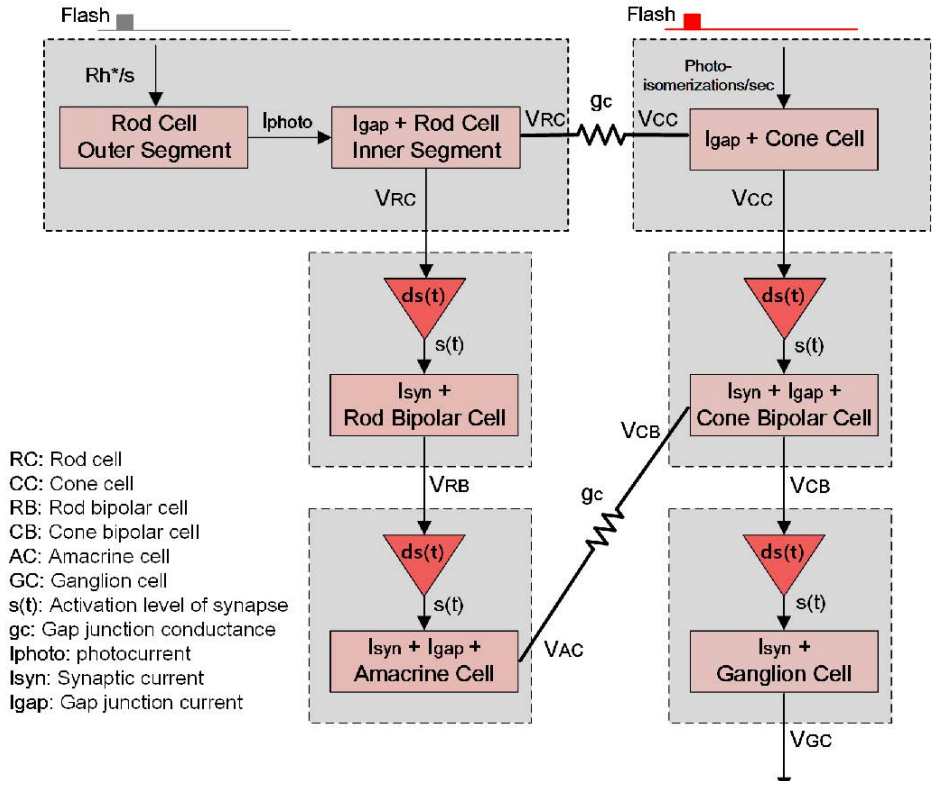

Figure2.3.2. Parallel signal flow pathway diagram.

instead of assuming the linear rate of visual field loss, this time it proceeds at the nonlinear rate, and the results from this method were utilized further for examining the mean and pattern standard deviations across various levels of damages in the visual field [18]. Figure 2 displays a high-level diagram of the retinal signal movement pathway.

The simulator has been developed in C++, Kst graphics and the Microsoft Foundation Class graphic interface. Usage on Windows 10 is suggested. To allow processing in real time. The computational solution checks a number of differential equation solvers for the midpoint system and the fourth-order Runge-Kutta (RK4) method (ODE15s, ODE45, ODE23s, ODE113). It was noticed that ODE45 and ODE113 needed way too short time steps to simulate in real-time to converge stability and specific solutions.

The ODE15s and ODE23s are also appropriate for stiff structures but only with crude error tolerances. ODE15s proved to be the quickest and most reliable MATLAB solver, but RK4 for fixed time phases was consistently quicker. The process RK4 was 18.8 percent faster than the ODE15s solver for the default time step1ms. As such, the RK4 approach is used in the simulator.

Figure 3 displays the simulation flow map where the model analysis and plotting processes are built to optimize the CPU usage where the number of physical threads is reduced. The simplicity for the lay individual was a core aspect of our simulation, such that our simulator can be operated locally without high-performance GPUs or CPUs.

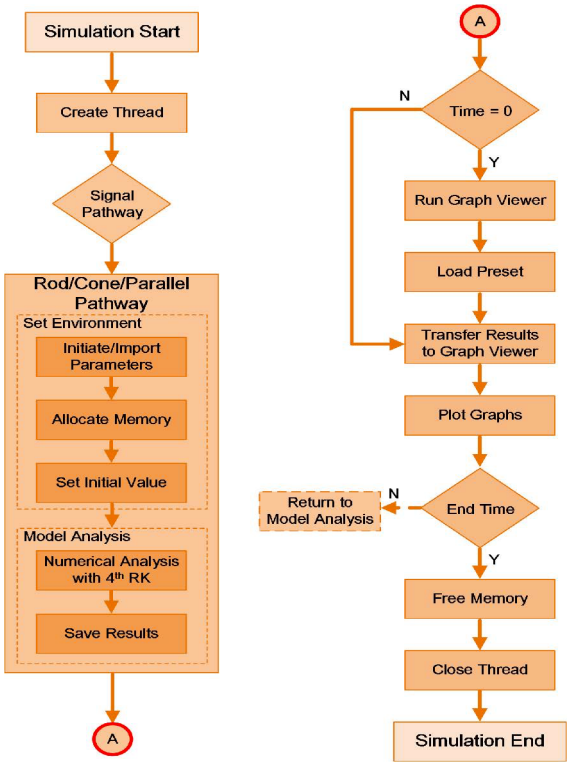

Figure 2.3.3. Fig. Retina simulator simulation flow map. Left: simulation continues the study of the model. Right: plotting the line to the conclusion of the simulation.

At the end, a discrete network retina simulator is proposed in this review. The simulator offers a simple and intuitive way for users to model different retinal cell dynamics and can reconfigure the cell parameters in the cascade and synaptic connections. This simulator is intended to provide neuroscientists and physiologists alike with more insight into the dependencies that occur between the many components of the retina. It can also be used by profound clinicians and engineers in biologically plausible learning to simplify the acquisition of retinal data that can be used to build more reliable models of neural coding and decoding in the visual cortex.

2.3.2 Detect the Presence of Glaucoma by LASER Radiation

[20] The goal of the research is to establish a new strategy for the early diagnosis of glaucoma through the temperature profiling of optic tissue with radiation from LASER. 3D CAD versions of the true human eye were used in the SolidWorks™ configuration and various parameters were calculated for the thermal simulation in COMSOL Multiphysics®, for three distinct LASER point sources: 694.3 nm of ruby LASER, 1064 nm Nd: YAG LASER, and 1340 nm Nd: yap LASER.

The main concept behind this technique was fluctuating temperature readings due to the presence of aqueous humor caused by increased intraocular pressure inside the human eye, resulting in increased resistance in the trabecular meshwork of glaucoma patients. A 3D model of the human eye and sources of irradiance has been created in solid works, whereas an external LASER source has been used for building up the temperature inside the human eye. During the simulation, pulse duration was kept between 0.5ms to 1.0ms while making sure that this duration doesn't beyond 1.0ms as it can complicate the readings. The results showed progressive visuals of glaucoma at 11 different stages. As the amount of aqueous humor increased, the temperature readings fell down. This inverse relation of glaucoma and temperature rise was compared with a theoretical reading of temperature's effect on the increase in aqueous humor, which became a successful parameter for glaucoma detection in further trials. The main objective of temperature profiling is to establish a new approach in the detection of glaucoma in the human eye. Simulations were created by 3D models of various light sources and the human eye. An example of this simulation can be found in figure 2.2.2.1

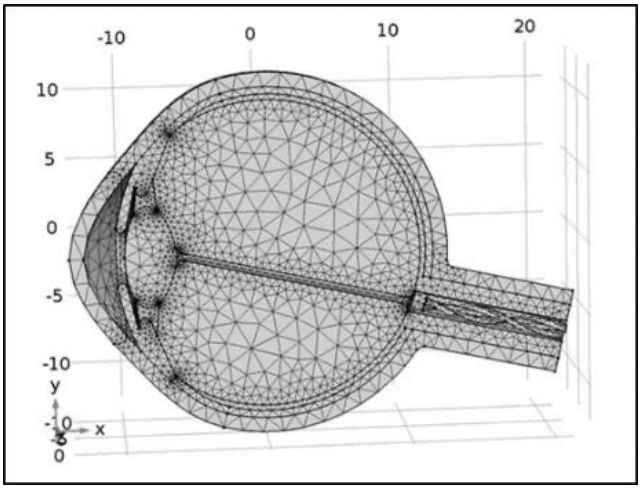

Figure 2.2.2.1: Geometric modelling (Three-dimensional)

The key aim of this work was to create a modern approach to the early diagnosis of glaucoma in the human eye. All the accompanying simulations have been carried out using 3D versions of the human eye and light sources. There was an interpretation of the simulated effects, and an inverse relationship between temperature variance by irradiated light with glaucoma progression was obtained, justified by the theoretical association between temperature and aqueous humor mass. This thesis also suggests Ruby LASER as a protected source of activation for temperature profiling. The shift of temperature attributable to irradiated light may be used as a parameter for the early diagnosis of glaucoma. Irreversible blindness and other complexities induced by glaucoma should not be removed. Treatment preparation would be better for glaucoma. Together with non-invasive eye thermal imaging (IR Thermography), this discovery may constitute a full diagnostic technique in the early stages of glaucoma diagnosis. This approach may be used

in other eye conditions, e.g. Macular degeneration correlated with age (AMD), diabetic retinopathy, cataracts, and glioma of the optical pathway, etc. Therefore, this approach may be called a benchmark identification procedure for the diagnosis of glaucoma and other ophthalmological disorders if effectively developed.

2.3.3 transcranial direct current stimulation (tDCS) analysis

[21] It could be difficult to modulate higher cognitive functions such as reading with tDCS, because reading includes regions in the dorsal and ventral cortical parts near to each other. The role of the dorsal pathway (mainly used to transform graph-phonologically) can interfere with ventral pathway function (used for semantics) if the two pathways are concurrently stimulated, and vice versa. In order to achieve functional precision in the tDCS, it is necessary to stimulate every direction per session such that the current diffusion through the cortical regions due to the two mounts is minimally overlapping.

For the experimental stage, a simulation-based methodology has been used which takes 10 simulations in two sessions, 5 for each of the two pathways. COSMETS2 software has been used for these simulations. However, the size of each electrode has been changed from each other to ensure that simulation stays diversified as it becomes crucial for attaining position and size parameters of anodes and cathodes to be in alignment with the defined values. The gained values from these tests were further used for the measurement of current and overlapping of coordinates along with the average magnitude of current density on each pathway. These findings were helpful in mitigating the ambiguity of the selection of montage before conducting this kind of test in further studies. Similarly, in another study, the identification of structural damage in the visual pathway of multiple

sclerosis (MS) patients is reviewed in [22]. This study achieved the characterization of all the abnormalities in structures of visual pathways with the help of MRI and coherence tomography. The methodology adopted for this study involved trials of 28 patients having a historical diagnosis of MS with or without VEP findings.

In this analysis, the montages analyzed were simulated in COMETS2, a tDCS toolbox focused on MATLAB. COMETS2, utilizing the finite-element procedure, evaluates the scale of the real density distribution across 35,057 cortical nodes derived from a built-in head model. The magnitude of the current density measured in each node is the norm in the x-y-z direction of current density values and is a typical modeling parameter. The built-in head model was imported to carry out simulations of the COMETS2 montages, and the electrodeposition, size and current strength were defined in the user interface. The normal current intensity of 2 mA was taken into consideration, as this is a regularly encountered maximum. After completing the simulation of the mounting, two important outputs, namely the XYZ matrix coordinates (35057 to 3), were obtained, representing the position of cortical nodes (consisting of x, y and z co-ordinates) in native headspace and their corresponding magnitude of the current density (MCD) matrix (35057 x 1). The native headspace matrix was mapped with the Fieldtrip toolbox in Talairach space. Use the Talairach client to define anatomical positions of XYZ coordinates (33857 to 3) mapped to Talairach space. The coordinates are seen in the space of Talairach as seen in Figure 2.2.3.1.

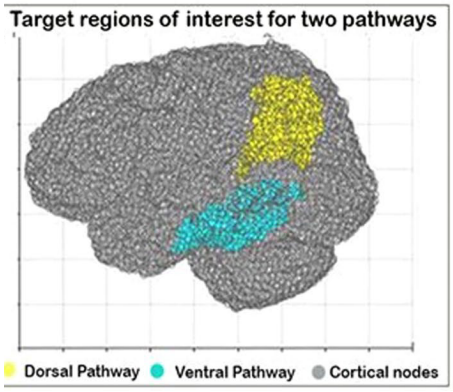

Figure 2.2.3.1. the position in Talairach space of the total number of nodes (grey color). The goal area of the dorsal (supramarginal gyrus) and ventral (center/lower temporal gyrus) are shown in yellow and cyanic colors.

The assumptions implicit in the model restrict all simulations of complex systems such as the MCD distribution. Therefore, it is essential to verify computational results utilizing neurophysiological findings. Although it is outside the reach of the current paper to verify the COMETS2 simulations, we notice that the findings obtained by the COMETS2 agree with those generated by the second ROAST simulation process. In addition, the method was established without respect to the existing flow path on the COMET2/ROAST MCD performance values. The conformity with a further criterion will consolidate the building blocks of the systemic methodology described in the present study. However only simulations had been left for future work.

2.3.4 Cerebral Cortex Simulations

A combination of comprehensive domain-specific expertise and appropriate software is needed to stimulate cerebral cortex simulation. However, in conjunction with that of the

program, the sophistication of the biological mechanism raises the risk of coding mistakes, thus slowing down model updates. In comparison, few life sciences are acquainted with software engineering and will benefit from flexibility in a high-level biological model abstraction. [23] The aim of this study is to construct a scalable frame for personal computers for cortical simulation. First of all, to separate an adjustable portion of the tech domain information. Then the system is built that reads the parameters of the model from comma value files and generates the code required for model simulations with Brian2. This distinction makes it easier to easily investigate complicated cortex circuits, thus reducing the probability of mistakes in coding by utilizing powerful hardware.

Methodology for developing the framework of CXsystem used comma-separated values (CSV) files which have the main body of user interface. The first file is called the model and network configuration file, having all the parameters required for building setup and anatomies of the proposed model. Whereas the second file is called configuration files, having the algorithms for local connection and biophysical parameters making an impact on the voltage of the cell membrane. The three components of the CXsystem have been constructor, parser, and physiology reference. Results were gathered by evaluating the CXsystem in three ways. The first procedure was to verify it using the COBAHH model, and the outcome of the software was compared with the referenced model called Brian 2. The second verification procedure was used for making a comparison between the performance of devices connected to CXsystem. The last approach was to test the weakness in scaling performance using independent clusters. The findings suggested that this proposed system did give the output involving all the goals of the original mode. However,

the improvement was seen in the form of minimized developing time as it was easy for users to understand. This system covers all the basic requirements of software exploring complex models in an efficient manner, facilitating the research in future work.

CXsystem user interfaces contain two comma-separated (CSV) files. First, the Cerebral Cortex Network Simulation Model and Managing Difficulty configuration file includes simulation setup parameters and the network anatomical layout of the model. This framework encompasses all interactions between cell types, their probability of interaction, and the number of synapses and connections. Second, the physiological configuration file includes both the proliferation of local contacts and all the biophysical parameters at the neuron and synapse stage concerning the membrane voltage. The input to stimulate the device today involves the thalamocortical spikes afferent with the user's defined timing. There are three principal components of the CXsystem: the CXsystem constructor, the parameter parser and the relation to physiology see Figure 2.2.4.1. The CXsystem Constructor reads and constructs anatomy in model and network setup. The parameter parser reads and extracts the physiological configuration file. These are presented with the connection to physiology, which collects all the elements needed to generate desired artifacts for Brian2. Next the guide in physiology packs the appropriate physiological parameters as a reference dictionary and passes them on to the CXsystem builders, the only access to the Brian2 simulator.

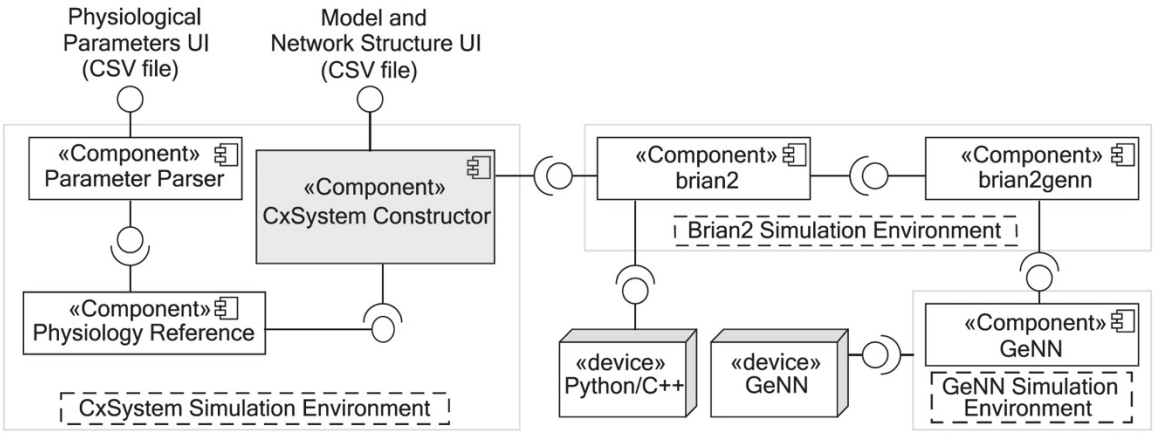

Figure 2.2.4.1. CXsystem 's UML diagram displaying association with CSV files, internal CXsystem modules, the Brian2 simulator, the front end of Brian2genn, and the GeNN simulator.

Brian2 provides native C++ code creation, while Brian2 requires a GeNN simulator for the development of unified system architecture (CUDA) code through the Brian2GeNN Front. The CXsystem is planned to fix the small shortcomings of the Brian2 functions from the standalone devices C++ and GeNN. The key disadvantage is the usage of a single network, the mystical network of brian2, because the interface of Brian2GeNN does not accommodate several networks.

CXsystem efficiency has been tested in three separate ways. first, CXsystem 's output was contrasted with native Brian2 using the COBAHH model. Second, the efficiency analysis of three CXsystem -supported devices: Python, C++, and GeNN. Finally, the slow scaling of several independent runs in a cluster is checked. The generalized model of the neocortical microcircuit was conducted in other tests.

2.3.5 unsupervised visually guided learning

Neurons encode the physical arrangement of visual artifacts in sequential stages of the primate ventral visual pathway. [2] This study investigates how these cell-feeding properties may evolve via unregulated visually directed learning through computer simulation. Specific neurons in the model are seen to use the statistical regularity and temporal consistency of visual feedback during exercise to develop fire properties comparable to V4 and TEO neurons. The neurons in V4 encode boundary contour element conformation at a single location within an object irrespective of where the object is on the retina, whereas the TEO neurons provide details from several boundary contour components. It goes beyond the simple identification of objects, where neurons merely react to the existence of an entity as a whole, yet have an invaluable base on which the brain will later identify the whole object.

Study 1, VisNet was conditioned on identical artificial visual artifacts as shown in Figure 2.2.5.1.

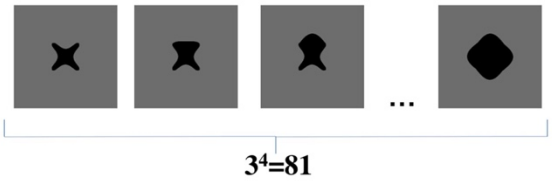

Figure 2.2.5.1 Shape of VisNet visual artifacts for study 1 preparation and research. Every entity has a fixed number of sides (n), each with a fixed number of potential boundaries (p).

For each simulation these visual artifacts had a fixed-sides number (n), and a set of boundary conformations or elements (p) was chosen for either of the two side curvatures,

and 256 pixels of virtual retina were predicted. Therefore, full objects were created from all combinations of (n x p) contour elements for each simulation. These artificially designed artifacts helped us to explore how n and p influence the learned neuronal answer. Then explored the creation of translation invariance when artifacts are moved 10 pixels over a grid of four separate positions on the retina using the above stated trace learning mechanism.

In Study 2, the VisNet visual stimuli are identical to the artificial stimuli used in the Pasupathy and Connor neurophysiological experiment (2001) seen in Figure 2.2.5.2.

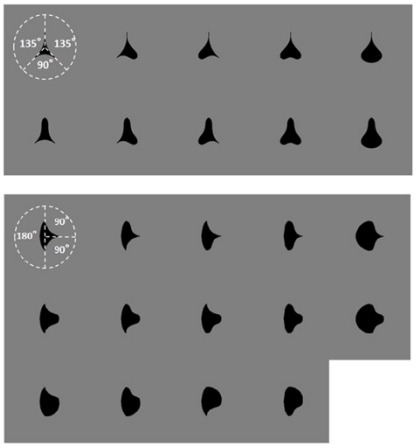

Figure 2.2.5.2 Type of visual objects used in VisNet Study2 preparation and research.

This allowed for a direct comparison among the neuronal reaction characteristics learned in the VisNet model and cell reactions experimentally controlled that encode local boundary results. The stimuli have been systematically generated by integrating sharp convex, medium convex, wide convex, medium concave, and broad concave border

components in order to shape closed forms. We also change the angular separation of the vertices for the stimulus at 256 x 256 pixels of the artificial retina, as shown in Figure 2.2.5.2. In addition, we also rotated the visual stimulation at a central position on the retina at a single step of 10 p.m. over the process of our testing to ensure more natural visual performance. This indicated that the statistical distinction between the boundary elements was not as clean as study 1. Nevertheless, we anticipated the sufficient statistical decoupling between the border elements with the new artifacts used in Study 2 to ensure that the network formed neurons during a visually directed learning phase that reacted to the localized boundary curvature. For all study 2 simulations, the VisNet design consisted of three layers of SOM, each consisting of (64 x 64) neurons per sheet. In the process of the training, the feed-forward synaptic weights are adjusted by using the trace learning rule to establish translational neuronal reactions.

Study3 trained VisNet with photos of natural objects to show that the learning processes explained in this paper and testing for real-world visual objects with artificially built visual stimulation in Study 1 and 2 parts are still successful. We presume that in many photos of natural objects with different boundary shapes an efficient statistical distinction would be formed between localized boundary components, which are described by the local curvature and the angular location with respect to the object's center of mass. This could cause the neurons in higher network layers to learn to react instead of to the entire objects to their individual boundary components. Figure 2.2.5.3 provides several representations of the real objects used in these simulations.

Figure 2.2.5.3. Pasupathy and Connor neurophysiological studies (2001). Examples of some of the practical visual artifacts used in Study3 for VisNet training.

The stimulus used in the simulations consists of 177 tridimensional realistic artifacts. Different forms of three-dimensional items are downloaded from the 3D Warehouse of Google, transformed to gray-scale models and revamped to the middle of 256 da 256 retinas. To strengthen the practical usage of visual images used to train VisNet, each natural object is rotated on a plane across 360 livres in steps of 10 livres during the training. When testing was done, neuronal responses were tested in the network with study 2 research stimuli Figure 2.2.5.2.

This paper shows that when the neural network model, VisNet, is trained in several artifacts with various frontier types on a primate ventral pathway, the neurons in the higher layers of the network will react to the localized contour elements, which are described by the curvature and the position of the border feature within the object reference frame. Interestingly, neurons learn to adapt to these restricting elements instead of to react to all objects introduced during training.

In addition, neurons were able to react with an invariance of translation as visual stimuli were passed across various retinal sites. This was active when VisNet was conditioned either by the visual stimulus used in studies 1 and 2 or by the pictures of real visual objects in study3.

Moreover, neurophysiological studies by others have shown that neurons from various boundary contour components combine the knowledge in the later stages of the ventral visual pathway, TEO, and posterior TE. In our simulations, the number of cells tuned to different contours in the higher layers increased. Backward the synaptic feed link with these output neurons verified that its selectivity was established by integrating neuron inputs representing each of the preceding layer's local boundary contours.

The VisNet design used in this paper included related learning only in the bottom-up (feed-forward) connections between successive network layers. In addition, the model did not include top-down relations, although they are understood to occur on the primate ventral route. In the present analysis, the reason for using this simpler architecture was that it is necessary to reproduce how neurons in V4, TEO and posterior TE learn to encode border contour element conformations at a specific location of an entity. Nevertheless, some related studies have shown that responses to neurons that have favored responses to orientated boundaries at early stages of visual perception such as V1 and V2, are modulated on either side of a diagram the edge appears. This is also the case when the figure/background markers lie well outside of the neuron's classical receptive region. This indicates that globally defining boundary ownership modulates neuronal function.

This contextual knowledge must be communicated to these visual neurons in the early phases by integrating the top-down layer connections with the repeated layer connections.

References

[1] P. D. Christine E.Collins, *THE PRIMATE VISUAL SYSTEM SYSTEM*. Taylor & Francis e-Library, 2005.

[2] A. Eguchi, B. Mender, B. Evans, G. Humphreys, and S. Stringer, "Computational Modelling of the Neural Representation of Object Shape in the Primate Ventral Visual System," *Front. Comput. Neurosci.*, vol. 9, p. 100, 2015, doi: 10.3389/fncom.2015.00100.

[3] M. J. Tovee, "An introduction to the visual system." Cambridge University Press, 2008.

[4] R. J. W. Mansfield, "Neural basis of orientation perception in primate vision," *Science (80-.).*, vol. 186, no. 4169, pp. 1133–1135, 1974.

[5] Z. Li, "A saliency map in primary visual cortex," *Trends Cogn. Sci.*, vol. 6, no. 1, pp. 9–16, 2002.

[6] S. W. Kuffler, "Discharge patterns and functional organization of mammalian retina," *J. Neurophysiol.*, vol. 16, no. 1, pp. 37–68, 1953.

[7] V. Bruce, P. R. Green, and M. A. Georgeson, *Visual perception: Physiology, psychology, & ecology*. Psychology Press, 2003.

[8] D. Saur *et al.*, "Ventral and dorsal pathways for language," *Proc. Natl. Acad. Sci.*, vol. 105, no. 46, pp. 18035–18040, 2008.

[9] T. C. Kietzmann, J. D. Swisher, P. König, and F. Tong, "Prevalence of selectivity for mirror-symmetric views of faces in the ventral and dorsal visual pathways," *J. Neurosci.*, vol. 32, no. 34, pp. 11763–11772, 2012.

[10] X. Cao, Y. Fang, L. Zhu, X. Li, and L. Zhang, "Research on Computational Simulation of Advertising Posters Visual Cognition," 2020, pp. 295–308.

[11] A. Eguchi, "Neural network modelling of the primate ventral visual pathway." University of Oxford, 2017.

[12] G. St-Yves and T. Naselaris, "The feature-weighted receptive field: an interpretable encoding model for complex feature spaces," *Neuroimage*, vol. 180, pp. 188–202, 2018.

[13] D. J. Kravitz, K. S. Saleem, C. I. Baker, L. G. Ungerleider, and M. Mishkin, "The ventral

visual pathway: an expanded neural framework for the processing of object quality," *Trends Cogn. Sci.*, vol. 17, no. 1, pp. 26–49, Jan. 2013, doi: 10.1016/j.tics.2012.10.011.

[14] J. M. Galeazzi, L. Minini, and S. M. Stringer, "The Development of Hand-Centered Visual Representations in the Primate Brain: A Computer Modeling Study Using Natural Visual Scenes," *Front. Comput. Neurosci.*, vol. 9, p. 147, 2015, doi: 10.3389/fncom.2015.00147.

[15] L. Hu, "Modeling of Visual Cognition, Body Sense, Motor Control and Their Integrations," 2017.

[16] E. T. (2008. Rolls, "Memory,Attention,andDecision Making.AUnifying ComputationalNeuroscienceApproach.," *Oxford:OxfordUniversityPress.*, 2008.

[17] A. J. Tatham, R. N. Weinreb, and F. A. Medeiros, "Strategies for improving early detection of glaucoma: the combined structure-function index," *Clin. Ophthalmol.*, vol. 8, pp. 611–621, Mar. 2014, doi: 10.2147/OPTH.S44586.

[18] S. Baek, J. K. Eshraghian, W. Thio, Y. Sandamirskaya, H. H. C. Iu, and W. D. Lu, "A Real-Time Retinomorphic Simulator Using a Conductance-Based Discrete Neuronal Network," in *2020 2nd IEEE International Conference on Artificial Intelligence Circuits and Systems (AICAS)*, pp. 79–83.

[19] T. Guo *et al.*, "Understanding the Retina: A Review of Computational Models of the Retina from the Single Cell to the Network Level," *Crit. Rev. Biomed. Eng.*, vol. 42, pp. 419–436, Jan. 2014, doi: 10.1615/CritRevBiomedEng.2014011732.

[20] S. Ghosh, M. Rabbani, and A. S. M. S. Arefin, "A Simulation Based Study for the Early Detection of Glaucoma Using Temperature Profiling of Human Eye," *Dhaka Univ. J. Sci.*, vol. 68, pp. 37–44, Aug. 2020.

[21] S. Bhattacharjee, R. Kashyap, B. Rapp, K. Oishi, J. E. Desmond, and S. H. A. Chen, "Simulation Analyses of tDcS Montages for the investigation of Dorsal and Ventral pathways," *Sci. Rep.*, vol. 9, no. 1, pp. 1–17, 2019.

[22] M. Pawlitzki *et al.*, "MS optic neuritis-induced long-term structural changes within the visual pathway," *Neurol. Neuroinflammation*, vol. 7, no. 2, 2020.

[23] V. Andalibi, H. Hokkanen, and S. Vanni, "Controlling complexity of cerebral cortex

simulations—I: CxSystem, a flexible cortical simulation framework," *Neural Comput.*, vol. 31, no. 6, pp. 1048–1065, 2019.